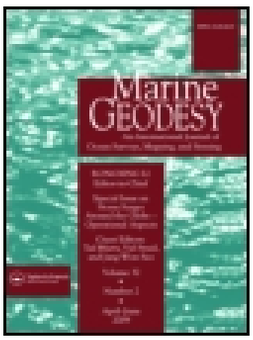

Marine Geodesy

ISSN: 0149-0419 (Print) 1521-060X (Online) Journal homepage: http://www.tandfonline.com/loi/umgd20

Analysing Uncertainty in Multibeam Bathymetric Data and the Impact on Derived Seafloor Attributes

Vanessa Lucieer, Zhi Huang & Justy Siwabessy

To cite this article: Vanessa Lucieer, Zhi Huang & Justy Siwabessy (2015): Analysing Uncertainty in Multibeam Bathymetric Data and the Impact on Derived Seafloor Attributes, Marine Geodesy, DOI: 10.1080/01490419.2015.1121173

To link to this article: http://dx.doi.org/10.1080/01490419.2015.1121173

Analysing Uncertainty in Multibeam Bathymetric Data and the Impact on Derived Seafloor Attributes

Vanessa Lucieer[1,*], Zhi Huang[2,$], Justy Siwabessy[2,#]

[1]University of Tasmania, Institute of Marine and Antarctic Studies, Hobart, Australia

[2]Geoscience Australia, Canberra, Australia

[*]Corresponding Author Email: vanessa.lucieer@utas.edu.au

[$]Corresponding Author Email: Zhi.Huang@ga.gov.au

[#]Corresponding Author Email: Justy.Siwabessy@ga.gov.au

Abstract

Multibeam bathymetric data provides critical information for the modelling of seabed geology and benthic biodiversity. The accuracy of these models is dependent on the accuracy of the bathymetric data which contains uncertainties that are stochastic at individual soundings but exhibit a distinct spatial distribution with increasing magnitude from nadir to the outer beams. A restricted spatial randomness method which simulates both the stochastic and spatial characteristics of the data uncertainty performed better than a complete spatial randomness method in analysing the impact of bathymetric data uncertainty on derived seafloor attributes.

1. Introduction

Shipboard multibeam echo sounders (MBES) have the capacity to create high resolution (e.g., sub-metre in very shallow water) maps of bathymetry (depth) and seabed morphology. In recent years we have continued to see advancement in MBES technology which has further enhanced an already valuable source of seafloor data. These advances have come out of traditional user groups extending the application of the data to meet new requirements and from the motivation of new user groups wanting to employ the technology. This wide ranging and ever growing community of MBES users are adapting and extending the potential of MBES data to address unique applications. MBES users have traditionally included hydrographers, navigators, engineers, marine geologists and military planners; but now we see the extension of the technology to meet the needs of maritime explorers, archaeologists, fisheries biologists, geomorphologists and ecosystem modelers to name a few. Bathymetry data and its derivatives have a range of applications that are relevant to supporting management of marine ecosystems. For example, bathymetry data can provide a potentially powerful physical surrogate for benthic biodiversity (e.g. Gogina 2010, McArthur et al. 2010) due to its relationship with light availability, food availability and water temperature. Similarly, morphological and seafloor terrain variables such as slope, aspect, Bathymetric Position Index (BPI), mean curvature and rugosity derived from bathymetry data through GIS analysis (Lundblad et al. 2006, Wilson et al. 2007, Liu et al. 2012) not only describe seabed morphology but can also act as proxies for oceanographic processes. Therefore they are often used as surrogates for the distributions of benthic species (e.g., Kostylev 2005, Holmes 2008, Huang 2012, Hill et al. 2014, Huang 2014).

The rapid rise in both the availability of MBES data, and methods for deriving seabed derivatives has coincided with a rapid expansion of marine protected area networks worldwide (Harris and Whiteway 2009). The management of these reserves requires inventories of benthic communities within marine reserves and an understanding of the role that habitat plays in the performance of the reserves in protecting these communities. In 2012, for example, the Australian Commonwealth government announced a Nationally Representative System of Marine Protected Areas within the Commonwealth jurisdiction (i.e. outside of the 3 nautical mile limit of state waters). This added more than 2.3 million km^2 of seabed to Australia's existing state and commonwealth marine reserves, taking the total area of seabed in commonwealth reserves, excluding the Great Barrier Reef Marine Park, to approximately 2.7 million km^2. Importantly, however, only 12.4 % of this area has been mapped by multibeam acoustics. The detailed seafloor morphology of the remaining 87.6 % is unmapped, and our understanding of the biological communities that this area supports is based solely on model-based predictions.

It will take many decades to map Australia's marine reserve network, and in the meantime reserve managers must continue to rely on model-based inventories of the biological communities that are likely to be present in these areas. These models form the basis against which changes in these communities, and hence the effectiveness of management regimes, are subsequently measured. Hence, not only is there a pressing need to gather additional seabed topography data, but also to understand the uncertainty in this data because of the implications this uncertainty has on model-based prediction of biological communities.

High resolution bathymetric data are useful to address one of the most critical issues in marine habitat mapping by modelling benthic habitat suitability and species distribution (Kostylev et al.

2003, Garza-Perez et al. 2004, McArthur et al. 2010, Rengstorf et al. 2012, Yesson et al. 2012, Cameron et al. 2014, Hill et al. 2014). Prediction models have been refined from hundreds of square kilometres (Kostylev et al. 2003, Iampietro 2008) to square meters (Monk et al. 2012). With this increase in resolution the reliability of the input spatial variables (derivatives of MBES bathymetry such as slope, curvatures, rugosity etc.) will come under close scrutiny when models are being validated. The quality of bathymetric data is a source of uncertainty which can impact on the success of the prediction model outputs. Indeed, the identification of the errors and relevant scales at which particular seabed morphological variables influence habitat selection may be as important as the selection of the spatial variables themselves (Mateo Sánchez et al. 2013). Recent studies (Foster et al. 2012, Foster 2014) also explored the implications of errors associated with non-colocated physical and biological data for spatially predicted covariate modelling. However, the relationships among the uncertainties in the bathymetric data and the derived spatial layers need to be completely understood in habitat suitability modeling.

There has been an increasing in attention to spatial uncertainty in MBES acoustic data representation (e.g., Hare et al. 1995, Lurton 2003, Lurton and Augustin 2010, Mosher 2011, Rengstorf et al. 2012, Dolan and Lucieer 2014). As the resolution of the data increases, the need for estimates of uncertainty also increases to verify the small scale seabed features that are *supposedly* being detected. Due to its high spatial resolution (e.g., roughly 1/50 of water depth), many users have assumed that multibeam bathymetry data are highly accurate in measurement. In reality, both vertical and horizontal uncertainties exist in every data point (or sounding). How to quantify these uncertainties and evaluate their impact on the subsequent products and models are important questions for the marine research community.

Until recently, much of the literature on acoustic uncertainty has been focused on the physical collection of sound profiles in the water column above the seabed (Mosher 2011, Lurton et al. 2012). This focus has left those who deal with MBES as a delivered product (e.g bathymetric raster) at a distance from being able to assess the quality of the acoustic data for their own particular purpose. In addition, as datasets are collected over time there need to be methods available to assess the utility of archived acoustic data for new applications from which it may not have initially been intended. As national mapping -SeaMap Tasmania (Jordan et al. 2005) and UKSeaMap (McBreen 2011) and international mapping MAREANO (http://mareano.no/en) initiatives increase, a method to assess the data for a fitness for use is required. We acknowledge that all forms of uncertainty are equally important. However, in this study we restrict the analysis to the propagation of *a priori* uncertainties in the digital elevation model (DEM). This uncertainty has greatest impact on the spatial derivatives which are used as the foundation data to seabed classification and characterisation.

1.1 Aims and technical scope

The aim of this study is to quantify the effects of *a priori* uncertainties in the digital elevation model (DEM) (or bathymetric surface) on three key derivatives: slope gradient, mean curvature and rugosity (Jenness, 2004). This aim will be addressed by quantifying the uncertainty in the DEM when deriving the error distribution model from the Combined Uncertainty Bathymetric Estimator (CUBE) (Calder and Mayer 2003, Calder and Wells 2006) using two different randomisation methods: (i) Complete Spatial Randomness (CSR) and; (ii) Restricted Spatial Randomness (RSR). All of the morphometric features are calculated using a 3 x 3 window. Slope

gradient represents the rate of elevation (or bathymetry) change. In this study it was calculated as the maximum rate of change in bathymetric value from the processing cell to the window. Curvature was calculated as the second derivative of the bathymetric surface (Moore et al. 1991). Rugosity was calculated as the ratio of surface area to planar area using Jenness algorithm (Jenness, 2004). Although there are different ways of calculating the slope and curvature variables, depending on the local approximation methods (e.g., Moore et al. 1991, Shary et al. 2002), in this study, these two variables were calculated using the algorithms by Horn (1981) (Burrough and McDonnell 1998, Dolan and Lucieer 2014).There are three types of errors in multibeam depth (bathymetry) measurements. The systematic errors should be removed by best survey practice and data calibration. The outliers have to be flagged and removed before final bathymetric surface generation. Finally, stochastic uncertainties have to be estimated. In this study, we are only concerned about the stochastic uncertainties. There are many sources of the stochastic uncertainties in depth and position measurements. This is because 1) MBES is a composite system; 2) each component of the system (e.g., motion sensor, gyro and GPS) has its own measurement uncertainty; 3) there are measurement uncertainties for the spatial offsets of these components. In addition, depth and position uncertainties are also due to measurement uncertainties in key environmental factors such as sound speed profile, tide and draft.

The Combined Uncertainty Bathymetric Estimator (CUBE) recently implemented in several multibeam processing software tools shows progress towards quantifying the above stochastic uncertainty in multibeam bathymetry data (Calder and Mayer 2003, Calder and Wells 2006). CUBE is a gridding algorithm based on *a priori* estimation of depth and position uncertainties. For each sounding, the *a priori* estimated vertical and horizontal uncertainties derived from the

sensors, the time latency and the offset measurements are combined into two measures: Horizontal Uncertainty and Vertical Uncertainty. CUBE then propagates these two combined uncertainties from individual soundings to each grid cell (node) using the equation below.

$$\sigma_p^{\,2} = \sigma_v^{\,2}\left(1+\left(\frac{d+hes\times\sigma_h^{\,2}}{res}\right)^{\alpha}\right)$$

Where $\sigma_p^{\,2}$ is the propagated uncertainty of the sounding after being translated to the node, $\sigma_v^{\,2}$ is the sounding's vertical uncertainty, $\sigma_h^{\,2}$ is the sounding's horizontal uncertainty, *d* is the distance from the sounding to the node, *hes* is the scale factor for worst expected horizontal uncertainty (typically equals to 2.95), *res* is the resolution of the grid (i.e., grid cell size), and α is the user specified distance exponent (typically equals to 2.0). The idea is for soundings that are closer to the node to have a smaller uncertainty contribution than those soundings that are far from the node. For each node, contributing soundings are processed one at a time. The first sounding forms a hypothesis (or an estimation) of depth. With more incoming soundings, either the hypothesis is updated or a new one forms. Consequently, multiple hypotheses of depth can be constructed for the node. Finally, the algorithm uses an uncertainty-weighted mean (a Bayesian estimator) to determine the best estimate of depth from these hypotheses and quantifies an uncertainty on the depth estimate (Calder and Wells 2006). It should be noted that this uncertainty value at each grid cell does not indicate the actual offset from the true depth but equal to one standard deviation of the uncertainty distribution (assuming a Gaussian distribution with zero mean).

To simulate the uncertainty magnitude and its spatial distribution within the multibeam bathymetry data surface, a randomisation process is required. Two randomisation methods i.e., CSR and RSR can be used for the process (Fortin 2005). The CSR, often implemented as the default method (or null model), regards data uncertainty in every grid cell as independent and assumes that the data uncertainty varies within a known statistical distribution without any neighbourhood effect (Fortin 2005). The RSR assumes spatial structure (e.g., spatial autocorrelation) in the data uncertainty (Manly 1997, Fortin 2000). By comparison, we would like to investigate whether the RSR is a superior randomisation method to the null model in the case of simulating the impact of the multibeam bathymetry data uncertainty.

An uncertainty propagation model is needed to investigate how the uncertainty in the multibeam bathymetry data, represented as the construction of the uncertainty surface, is propagated through to the derivatives. The Monte Carlo (also known as stochastic) simulation method has been recognised as an uncertainty analysis technique in a number of terrestrial studies (Heuvelink 1998, Canters and De Genst 2002).The Monte Carlo simulation model is suitable for our purpose because it is theoretically applicable to any function including the GIS operations implemented in this study (Openshaw 1991, Heuvelink 1998, De Genst et al. 2001, Oksanen and Sarjakoski 2005, Huang 2009, Dolan and Lucieer 2013).

The residual uncertainties of any MBES system can be expected to vary from about 5-10 cm to over 30 cm in places, increasing with depth (Fonseca and Mayer 2007). Given many hydrographers preference it to use the outer-beam soundings from MBES, the practical effect of residual uncertainty could be that this variation could be significantly greater than 30 cm. In

shallow water (< 50 m), this can easily be in the order of 1-2 % of depth (Vasquez 1999). The Monte Carlo simulation creates multiple input bathymetric surfaces (DEM) that can be used as equally probable input layers to calculate spatial derivatives. The slope, curvature and rugosity are the most commonly used spatial derivatives utilised in community distribution modelling. These parameters not only effectively describe the relief and structure of the seafloor but can also describe how exposed the seafloor can be to prevailing currents and explain why particular seabeds might make preferential habitat for different communities.

2. Methods

2.1 Study Site

We present a case study from a survey of the Oceanic Shoals Commonwealth Marine Reserve (CMR) in the Timor Sea (Australia), conducted by the Marine Biodiversity Hub through the Australian Government's National Environmental Research Program (Nichol 2013). The study area is characterised by steep carbonate banks and terraces with abrupt breaks in slope of limited spatial extent (Figure 1). The carbonate banks and terraces are important habitats of biological diversity because they provide the hard ground required for diverse epibenthic assemblages of sponges and corals, with their steep flanks marking the environmental transition to deeper water, characterised by soft sediment habitats. In this region, the continental shelf is characterised by a wide low-gradient ramp with sandy bioclastic sediments reflecting both the modern biota and the sea level fluctuations coupled with present-day oceanographic processes. The bioclastic sediments are represented by a mixture of modern bioclasts, marine deposits stranded by sea-level rise and precipitated carbonate grains (ooids and peloids), which were formed prior to the

establishment of the Indonesian Through, about 12ky B.P. (Collins 2011). The atolls are north – south oriented and are pear-shaped, with the narrow end towards the north west. The shoals rise with nearly vertical sides to water depths of 30 m from 170 m of water depth.

2.2 Bathymetric data.

Multibeam bathymetric data was acquired using a Kongsberg EM3002D (300 kHz) sonar system mounted in single head configuration. The multibeam data were processed using Caris HIPS & SIPS v7.1 software (CARIS 2013). The processing of the bathymetric data has been carried out according to the following steps: i) applying algorithms that corrected for tide and vessel pitch, roll and heave (e.g. elevation errors caused by dynamic draft of the vessel); ii) sound velocity profiles (collected whilst underway and at several stations in each survey area) to correct for variations in the speed of sound through the water column and; iii) software filters and visual inspection of each swath line to remove artefacts and noisy data (e.g. nadir noise and data outliers) where possible. The final bathymetry grid was generated from the CUBE algorithm and gridded at 2 m spatial resolution in order to construct the DEM of the study area (Figure 1). This bathymetric grid represents the best estimate of depth at each grid cell. The CUBE algorithm also generated an uncertainty layer that represents one standard deviation of the depth *a priori* uncertainty at each grid cell (Figure 2). The uncertainty layer shows that the standard deviation of the depth uncertainty at each grid cell ranges from 0.31m to 0.60m. The uncertainty layer also shows a clear spatial pattern with depth and a gradual increase from the nadir to outer beams (Table 1).

2.3 Randomisation methods

Two randomisation methods were used to construct different models of the depth uncertainty surface. The CSR method assumed that the depth uncertainty varies independently at each grid cell. It also assumed that the uncertainty distribution at each grid cell follows a Gaussian distribution with a mean equal to zero and a standard deviation equal to the uncertainty value obtained from the CUBE uncertainty layer (Figure 2). For each grid cell independently, a random number generator was used to calculate a depth uncertainty value from the Gaussian distribution.

The RSR method recognised distinct spatial structures in the depth uncertainty distribution, indicated by the uncertainty layer (Figure 2). The uncertainty layer indicates 28 levels of depth uncertainty ranging from 0.31 m to 0.60 m and increasing from the nadir to outer beams (Figure 2; Table 1). In this study, we denoted them as U_1, U_2, ••••••, U_{28}. The purpose of the RSR method was to maintain this spatial structure when constructing realisations of the depth uncertainty surface. To do that, we decided that each realisation of the depth uncertainty surface should contain exactly 28 levels of values each corresponding to a depth uncertainty level. On the depth uncertainty surface, the locations that have a lower depth uncertainty level (e.g., U_1) should have a depth uncertainty value smaller than those that have a higher depth uncertainty level (e.g., U_2) so that the spatial structure displayed in the CUBE uncertainty layer (Figure 2) can be maintained. For each realisation, we calculated the 28 depth uncertainty values, denoted as X_1, X_2, ••••••, X_{28}, according to the 28 depth uncertainty levels using the steps below:

1. X_1 = random.normalvariate(0,U_1=0.31),
2. X_{28} = random.normalvariate(0,U_{28}=0.60), and

3. X_2 to X_{27} were calculated using the following linear decay function:

$$X_i = \frac{(X_{28} - X_1)}{0.29} \times U_i + \frac{(0.60 \times X_1 - 0.31 X_{28})}{0.29}$$

Where i = 2, 3, ••••••, 27; U_i = 0.32, 0.33, ••••••, 0.58 (Table 1).

We do not know the actual relationship between depth uncertainties versus beam angles. The depth uncertainty levels (Figure 2 and Table 1) do indicate a linear increase of the actual depth uncertainties from the nadir to outer beams (e.g., U_1=0.30 m to U_{28}=0.60 m). Therefore we assumed that the actual depth uncertainties (X_1 to X_{28}) have also linear relationships with the depth uncertainty levels. As a result, we chose the linear decay function to calculate X_2 to X_{27}.

Two additional conditions were enforced for the implementation of the above steps (e.g., the random process would restart if the conditions were not met):

1) $X_{28} > X_1$, and
2) X_{28} and X_1 have the same sign (i.e., both positive or both negative).

To construct a depth uncertainty surface, each grid cell was assigned one of the 28 depth uncertainty values according to its uncertainty level. For example, if the grid cell has a depth uncertainty level of U_1, it will be assigned a value of X_1.

2.3 Monte Carlo Simulation

The depth surfaces are perturbed to create a new DEM realisation that yielded a probability distribution of possible outcomes. Monte Carlo simulation has been commonly used to analyse the propagation of error through simulating a set of modelled maps where grid cell values are

imputed with a random error drawn from an error model (Oksanen and Sarjakoski 2005, Lindsay 2006, Oksanen and Sarjakoski 2006, Hengl 2010). Many models (e.g. 100+) are computed to assess the impact of vertical error on subsequent digital elevation model (DEM) derivatives. In this study, the Monte Carlo simulation was implemented for 500 iterations (Figure 3). For each of these models the derivatives of slope, curvature and rugosity (Horn 1981, Jenness 2004) were calculated. Parameters such as the mean and standard deviation (S.D.) were calculated from these realisations and used to assess both the expected results of the model and the uncertainty associated with the inputs.

The diagram in Figure 3 shows the technical procedure of the Monte Carlo simulation which is summarised as follows:

1. to use both the CSR and RSR method to construct a realisation of the depth uncertainty surface,

2. to introduce the depth uncertainty surface to the bathymetry grid obtained from the CUBE algorithm (Figure 1) to obtain a perturbed bathymetry surface,

3. to derive a) curvature (CV), b) slope gradient (SG) and c) rugosity (RU) layers from the perturbed bathymetry surface using ArcGIS' "Surface" toolset and Jenness (2004) algorithm (e.g., rugosity = (true) surface area / grid cell size), and

4. to repeat the above steps 500 times.

The diagram also shows that for every set of 20 iterations we calculated mean and standard deviation layers from all of the current individual derivative layers using the ArcGIS' "cell statistics" tool. For example, SG20_m and SG20_sd denote the mean and standard deviation layers of the first 20 slope gradient layers; SG40_m and SG40_sd denote the mean and standard deviation layers of the first 40 slope gradient layers; while, SG500_m and SG500_sd denote the mean and standard deviation layers of all 500 slope gradient layers. As a result, we obtained 25 mean layers and 25 standard deviation layers for each derivative.

We calculated the absolute differences between the adjacent mean (or standard deviation) layers cell by cell (e.g., SG40m and SG20m) in order to evaluate the convergence of the Monte Carlo simulation. The spatial means of the 24 difference layers were plotted to show whether the differences were reduced and eventually converged with the increase of the iterations. The convergence threshold was calculated as 20% of the difference between the maximum mean difference and the minimum mean difference. We considered the Monte Carlo simulation converged when the consecutive mean differences were smaller than the convergence threshold from the converging iteration to the 500^{th} iteration.

3. Results

The results of the randomisation processes have shown that the CSR and RSR methods construct very different depth uncertainty surfaces (Figure 4). A snapshot at the 100th iteration shows the depth uncertainty surface generated by the CSR method exhibiting no spatial pattern across a depth uncertainty range of -2.6 m to 2.58 m (Figure 4A). In contrast, the depth uncertainty surface generated by the RSR method shows clear spatial patterns with uncertainty increasing

from the nadir to the outer beams (Figure 4B). This pattern is very similar to that of the CUBE generated uncertainty layer (Figure 2). The contrast in the spatial patterns of the CSR and RSR uncertainty surfaces clearly demonstrates the ability of the RSR method to maintain the realistic spatial structures in the CUBE's uncertainty layer.

For the CSR method, the Monte Carlo convergence lines for all three derivatives and two statistics (mean and standard deviation) show a continuous decrease of corresponding values. A sharp decrease followed by a gradual decrease was observed (Figure 5). For the curvature and slope gradient variables, the Monte Carlo simulation converged after 180 and 160 iterations for the mean and standard deviation statistics, respectively (Figure 5A-D). For the rugosity variable, the Monte Carlo simulation converged after 180 iterations for both statistics (Figure 5E & F).

The Monte Carlo convergence lines are more complex for the RSR method (Figure 6). Nevertheless, a general declining trend could be observed. For the curvature variable, the convergence line of the mean statistic shows a very sharp initial decline, followed by a gradual increase, until it converges after 160 iterations (Figure 6A). The convergence line of the standard deviation statistic varies until it converges after 300 iterations (Figure 6B). Similar patterns occurred for the Monte Carlo simulation of the slope gradient variable (Figure 6 C&D). For the rugosity variable, the mean statistic again shows steep initial decrease followed by gentle decrease and an up-and-down, before converging after 160 iterations (Figure 6E). The same could be observed for the standard deviation statistic (Figure 6F).

Comparing Figure 6 with Figure 5 reveals the impact of the different scenarios of uncertainty simulation would have on the Monte Carlo method. Complete randomness simulated by the CSR

method was simplistic. In addition to the non-spatial stochastic uncertainty, the RSR method also simulated the spatial structure of the depth uncertainty. Although this spatial structure has a general pattern of increasing uncertainty from nadir to outer beams along the east-west survey lines, at some areas (e.g., northern part of the study area) the uncertainty pattern is more complex (Figure 2). These two levels of complexity, we believe, were the reasons for the more complex Monte Carlo convergence. This was especially true for the standard deviation statistic, which generally experienced more up-and-down and converged later than the mean statistics (Figure 6B&D vs Figure 6A&C), likely because it lacks the smoothing effect of mean statistic.

The curvature variable (Figure 7A) was derived from the unperturbed bathymetric grid obtained from the CUBE algorithm (denoted CV). Figure 7B displays the mean curvature layer after 500 iterations of the CSR method (e.g., CV500_m). It appears to be noisy, although the main features identifiable from Figure 7A are still discernable such as the break in slope at the edges of banks and terraces. On the other hand, the CV500_m layer obtained from the RSR method (Figure 7C) is clearly more similar to Figure 6A. The absolute differences between the two CV500_m layers and the CV layer are shown in Figures 7D&E. The CSR method clearly resulted in much larger differences in the curvature variable than the RSR method. The overall difference was two magnitudes larger from the CSR method than from the RSR method (e.g., 1.517 Vs 0.015).

Figure 8A displays the slope gradient variable derived from the (unperturbed) bathymetry grid (denoted SG). Figure 8B displays the mean slope gradient layer after 500 iterations of the CSR method (e.g., SG500_m). The spatial pattern is very different from that of the unperturbed pattern shown in Figure 8A. Details for large areas of gentle and moderate slope gradient have

disappeared. In fact, the CSR method resulted in higher slope gradient at most locations. In contrast, the SG500_m layer obtained from the RSR method (Figure 8C) has a very similar spatial pattern to that of Figure 8A. The absolute differences between the two SG500_m layers and the SG layer are shown in Figures 8D&E. The CSR method clearly resulted in much larger differences in the slope gradient variable than the RSR method. The overall difference was two magnitudes larger from the CSR method than from the RSR method (e.g., 4.511^{o} Vs 0.034^{o}).

Figure 9A displays the rugosity variable derived from the unperturbed bathymetry grid (denoted RU). Figure 9B displays the mean rugosity layer after 500 iterations of the CSR method (e.g., RU500_m). The spatial pattern is very different from that Figure 9A. Again, the CSR method resulted in the removal of large areas of seafloor with low rugosity from the data. On the other hand, the RU500_m layer obtained from the RSR method (Figure 9C) has very similar spatial pattern to the unperturbed slope gradient layer (Figure 9A). The absolute differences between the two RU500_m layers and the RU layer are shown in Figures 9D&E. The CSR method clearly resulted in much larger differences in the rugosity variable than the RSR method. The overall difference was three magnitudes larger from the CSR method than from the RSR method (e.g., 0.069 Vs 0.00004).

Compared to the RSR method which had little impact on the realistic seafloor morphological patterns, the CSR method has significantly distorted the patterns (Figures 7-9); although this is visually less so for the seafloor curvature. This indicates that realistic spatial structure in the depth uncertainty distribution is important and must be accounted for uncertainty analysis. Simply applying the null model of the CSR method could result in unacceptable results.

Consequently, this would justify the effort to understand the nature and characteristics of data uncertainty prior to any subsequent analysis.

4. Discussion and Conclusions

Bathymetric data is significant to all ocean management decisions such as identifying living and non-living ocean resources, safe navigation, responding to extreme events, spatial planning and geohazard assessment. A fundamental limitation to effective marine management in Australia (and internationally), is the lack of continuous fine scale bathymetric information across its whole jurisdiction, which given its expanse at 9 million square kilometres (excluding the extended continental shelf) is an improbable task. The multibeam data that therefore is collected and available for the prediction of seabed substrates and species prediction modelling must therefore be quantifiably reliable and be able to be assessed for fitness for use. Monitoring and change detection of the seafloor requires detailed baseline data with uncertainty estimates to ensure that features that display change are reliably detected. The accuracy of marine habitat maps and their associated levels of uncertainty are extremely hard to convey visually or to quantify with existing methodologies.

The aim of this paper was to explore an accessible, practical tool and spatial analysis technique to quantify uncertainty in MBES data and explore the effects of uncertainty on the common bathymetric spatial derivatives of slope, aspect and curvature. By far the most common variables used in marine habitat prediction models are depth, seafloor morphology (e.g. slope, curvature, rugosity *etc.*), and sea surface temperature. The implications of the results of this analysis can provide invaluable information to policy and decision makers to get a sense of the accuracy of the common data source that is used to characterise our oceans and predict the distribution of

species. Understanding uncertainty in marine habitat mapping and its propagation during data manipulation and modelling is becoming one of the major issues in marine spatial analysis- the outcome of which can only lead to improved subsequent management decisions

MBES bathymetric data has notable uncertainties (Figure 2). There is a variety of sources for these uncertainties which will be propagated in subsequent derivative analysis and they can have different degrees of impact. At individual sounding locations, after data processing and cleaning, depth uncertainty is stochastic in nature. But over a survey area, it can increase as a factor of water depth and distance from the nadir, and therefore exhibit a distinct spatial pattern (Figure 2). The RSR method was able to simulate both the stochastic and spatial characteristics of the multibeam bathymetry data uncertainty (Figure 4B). Whilst the CSR method captured only stochastic uncertainties it did not characterise the spatial structure (Figure 4A). The results demonstrate that the RSR method is a much more realistic randomisation method for the *a priori* uncertainty analysis of multibeam bathymetry data than the CSR method. The results from the RSR method show that the uncertainty within the multibeam bathymetry has only a small impact on its three derivatives (Figures 7C&E, 8C&E, 9C&E). On the contrary, the CSR method exaggerated the uncertainty influence on the derivatives (Figures 7B&D, 8B&D, 9B&D).

This study confirms that the Monte Carlo method is appropriate for simulating the uncertainty propagation through GIS operations (e.g., (De Genst et al. 2001, Oksanen and Sarjakoski 2005, Dolan and Lucieer 2013). The procedures used to derive slope gradient, curvature and rugosity variables from the bathymetric DEM and their error propagation cannot be represented as simple mathematical functions. This rules out the application of formal mathematical models such as the Taylor analysis (Taylor 1982) for simulation. The Monte Carlo simulation method is flexible and

easy to implement in ArcGIS (Heuvelink 1998). In this study, the simulation of the CSR method demonstrates an ideal situation where the simulation quickly converged after less than 200 iterations with respect to the derivatives and statistics (Figure 5). The simulation of the RSR method was more complex with several fluctuations, especially for the standard deviation statistic (Figure 6). This is likely due to the fact that the spatial pattern of the stochastic uncertainties adds complexity to the Monte Carlo simulation.

In summary, the results of this analysis indicate that:

1. Multibeam bathymetry data *a priori* uncertainties are stochastic at individual soundings but exhibit a distinct spatial distribution with increasing distance from the nadir to outer beams.

2. The RSR method is able to realistically simulate both the stochastic and spatial characteristics of the data uncertainty.

3. The Monte Carlo method is appropriate for the uncertainty analysis of GIS operations.

4. Although multibeam bathymetry data have notable overall uncertainty level, its impact on subsequent derivative analysis is likely to be minor in this dataset at the 2 m scale.

The final multibeam bathymetric grid produced from MBES data is a modelled representation of the seafloor that contains inherent uncertainties. Understanding the structure and distribution of uncertainty in the DEM output is important as this uncertainty propagates into spatial analysis procedures in the workflow- from data acquisition to habitat map. However, the most practical application for understanding uncertainty in MBES products is that it allows resource managers to identify the cost effectiveness of error reducing strategies, such as increasing data sampling

over particular features of interest or improving the resolution of the data over a site using a specific sampling regime (such as waiting for improved weather conditions, remapping, increasing swath overlap etc.).

The result of this analysis has broader implications for ecological research such as modelling benthic fauna relationships to fine scale topographic features (Brown et al. 2011). We need to be able to assess the accuracy of sonar representation of these features within the bathymetric DEM or within the spatially derived products. The uncertainty in the bathymetric DEM will also impact the delineation of geomorphic features and/or derived quantitative descriptors of the seabed, such as slope or rugosity. The implications of uncertainty in the derived bathymetric products are also highly relevant for hydrodynamic modelling where much effort is invested in the precision of the acoustic measurements for modelling fine scale seabed features such as sedimentary bedforms. This important point comes full circle when the outputs of hydrodynamic modelling, which themselves incorporate bathymetry data are used as an input to benthic habitat modelling, on local or regional scales.

The results of this analysis can also influence species prediction models. These models provide a method by which continuous species distribution maps can be produced from limited (point) sampled data (Hill et al. 2014). This method is pertinent to both conservation studies and fisheries research, and is particularly useful in the deep sea where a number of biological communities have been identified as vulnerable 'habitats'. These models require an understanding of the factors influencing species distribution and abundance at different scales and how the use of multiple scales of seafloor bathymetry in the spatial analysis can improve the

model accuracy. If not treated properly, uncertain geomorphic classifications could be misleading as a predictor variable for benthic habitat in these models. Mellin et al. (2011)(states that if the design of a marine reserve is based on surrogate data (e.g terrain variables), it is vital to account for the uncertainty in the biodiversity predictions based on the type of surrogates used, as this could make the difference between extinction and persistence.

Reliable bathymetric data are fundamental for predictive modelling of water currents and circulation patterns, which in turn are used to inform environmental impact assessments and understand the degree and extent of ecological linkages between different areas (e.g. larval dispersal). Accurate bathymetry can also be used as a surrogate to infer habitat types for broad-scale benthic biodiversity mapping where ecological field data are limited. The ability to assess the quality and accurate scale of bathymetric data to fulfil objectives for monitoring biodiversity in Australian Commonwealth waters has come under review in the past year. This comes as Australia seeks to design, implement and test ways to integrate new and existing survey and monitoring methods in Commonwealth reserves around Australia. The development of methods to assess uncertainty in seafloor morphology data directly result from the assessment of survey designs and the need to develop biodiversity metrics that reflect the spatial variation in species group indicators (keystone species) of ecological health, and the impact of survey design on the variance and bias on collected data.

If keystone species are identified as being associated with a narrow or specific morphological feature on the seafloor it is necessary to know what the uncertainties in identifying this feature would be from the different MBES data layers across survey locations in Commonwealth waters. Due to the condition of MBES data uncertainties varying over time and space within and

between survey periods, there may be datasets which are subject to greater uncertainties than others. One of the major challenges in analysing time series of MBES data is maintaining internal consistency of acoustic processing methodology, especially in the face of technological changes. The seabed mapping community require a toolkit of methods to generate spatial maps of the uncertainties within a bathymetric DEM to help in the validation of subsequent benthic habitat maps. Uncertainty propagation should not be neglected and needs attention when developing systems that merge different sensor types or same data types over different time periods (Aitken et al. 2010). The results of this study will enable scientists and mangers to understand and interpret the outcome of uncertainty analysis for acoustically generated maps of benthic marine environments.

Acknowledgements

This work was undertaken for the Marine Biodiversity Hub, a collaborative partnership supported through funding from the Australian Government's National Environmental Research Program (NERP). NERP Marine Biodiversity Hub partners include the Institute for Marine and Antarctic Studies, University of Tasmania; CSIRO, Geoscience Australia, Australian Institute of Marine Science, Museum Victoria, Charles Darwin University and the University of Western Australia. Comments from the anonymous reviewers have improved the manuscript. This paper is published with permission of the Chief Executive Officer, Geoscience Australia.

References

Aitken, J., V. Ramnath, V. Feygels, A. Mathur, M. Kim, J. Y. Park and G. Tuell (2010). "Prelude to CZMIL: seafloor imaging and classification results achieved with charts and the rapid environmental assessment (REA) processor. Algorithms and technologies for multispectral, hyperspectral, and ultraspectral imagery Xvi." Spie-International Society for Optics and Engineering, 1: 7695.

Brown, C. J., S. J. Smith, P. Lawton and J. T. Anderson (2011). "Benthic habitat mapping: A review of progress towards improved understanding of the spatial ecology of the seafloor using acoustic techniques." Estuarine, Coastal and Shelf Science 92(3): 502-520.

Burrough, P. A. and R. A. McDonnell (1998). Principles of Geographical Information Systems. Principles of Geographical Information Systems. USA, Oxford University Press.

Calder, B. R. and L. A. Mayer (2003). "Automatic processing of high-rate, high-density multibeam echosounder data." Geochmistry Geophysics Geosystems 4: 1048.

Calder, B. R. and D. E. Wells (2006). CUBE User Guide. U. o. N. H. (UNH), Center for Coastal and Ocean Mapping (CCOM)/Joint Hydrographic Center (JHC)**:** 46.

Cameron, M., V. Lucieer, N. S. Barrett, C. R. Johnson and G. J. Edgar (2014). "Understanding community-habitat associations of fishes across temperate reefs in Tasmania using fine-resolution, bathymetry derived measures of physical habitat." Marine Ecology Progress Series 506: 213-229.

Canters, F. and W. De Genst (2002). "Assessing effects of input uncertainty in structural landscape classification." International Journal of Geographical Information Science 16(2): 129-149.

CARIS (2013). Caris HIPS and SIPS 8.1 User Guide. New Brunswick, Canada.

Collins, L. B. (2011). "Geological Setting, Marine Geomorphology, Sediments and Oceanic Shoals Growth History of the Kimberley Region." Journal of the Royal Society of Western Australia. 94: 89-105.

De Genst, W., F. Canters and H. Gulinck (2001). "Uncertainty Modelling in Buffer Operations Applied to Connectivity Analysis." Transactions in GIS 5: 305-326.

Dolan, M. and V. Lucieer (2013). The new wave of bathymetry data- uses and limitations for marine benthic habitat mapping and geomorphology. Geohab (Marine Geology and Benthic Habitat Mapping). Rome, Italy, Italian Geological Survey.

Dolan, M. F. J. and V. L. Lucieer (2014). "Variation and Uncertainty in Bathymetric Slope Calculations Using Geographic Information Systems." Marine Geodesy 37(2): 187-219.

Fonseca, L. and L. Mayer (2007). "Remote esimation of surficial seafloor properties through the applicaiton of Angular Range Analysis to multibeam sonar data." Marine Geophysical Research 28: 119-126.

Fortin, M.-J., Dale, M., (2005). Spatial Analysis: A Guide for Ecologists. Cambridge., Cambridge University Press.

Fortin, M.-J., Jacquez, G.M (2000). "Randomization tests and spatially autocorrelated data." Bulletin of the Ecological Society of America 81: 201-205.

Foster, S. D., Hosack, Geoffrey R., Hill, Nicole A., Barrett, Neville S., Lucieer, Vanessa L. (2014). "Choosing between strategies for designing surveys: autonomous underwater vehicles." Methods in Ecology and Evolution 5 (3): 287-297.

Foster, S. D., H. Shumadzu and R. Darnell (2012). "Uncertainty in spatially predicted covariates: is it ignorable?" Applied Statistics 61(4): 637-652.

Garza-Perez, J. R., A. Lehmann and J. E. Arias-Gonzalez (2004). "Spatial prediction of coral reef habitats: integrating ecology with spatial modelling and remote sensing." Marine Ecology Progress Series 269: 141-152.

Gogina, M., Glockzin, M., & Zettler, M.L. (2010). "Distribution of benthic macrofaunal communities in the western Baltic Sea with regard to near-bottom environmental parameters. 1. Causal analysis." Journal of Marine Systems, 79: 112-123.

Hare, R., A. Godin and L. Mayer (1995). Accuracy estimation of Canadian swath (multibeam) and sweep (multi-transducer) sounding systems. Canadian Hydrographic Service.Harris, P. T. and T. Whiteway (2009). "High seas marine protected areas: Benthic environmental conservation priorities from a GIS analysis of global ocean biophysical data." Ocean & Coastal Management 52(1): 22-38.

Hengl, T., Heuvelink, G.B.M., van Loon, E.E (2010). "On the uncertainty of stream networks derived from elevation data: the error propagation approach." Hydrology and Earth System Sciences 14: 1153-1165.

Heuvelink, G. B. (1998). "Uncertainty analysis in environmental modelling under a change of spatial scale." Nutrient cycling in Agroecosystems 50: 255-264.

Hill, N. A., V. Lucieer, N. S. Barrett, T. J. Anderson and S. B. Williams (2014). "Filling the gaps: Predicting the distribution of temperate reef biota using high resolution biological and acoustic data." Estuarine, Coastal and Shelf Science 147: 137-147.

Holmes, K. W., van Neil, K.P., Radford, B., Kendrick, G.A., Grove, S.L. (2008). "Modelling distribution of marine benthos from hydroacoustics and underware video." Continental Shelf Research 28: 1800-1810.

Horn, B. (1981). Hill shading and the reflectance map. . Proceedings of the IEEE.

Huang, Z., Laffan, S.W., (2009). "Sensitivity analysis of a decision tree classification to input data errors using a general Monte Carlo error sensitivity model,." International Journal of Geographical Information Science, 23: 1433-1452.

Huang, Z., McArthur, M., Przeslawski, R., Siwabessy, J., Nichol, S., Brooke, B., (2014). "Predictive mapping of soft-bottom benthic biodiversity using a surrogacy approach. ." Marine and Freshwater Research 65: 409-424.

Huang, Z., Nichol, S., Daniell, J., Siwabessy, P.J.W., Brooke, B.P., (2012). "Predictive modelling of seabed sediment parameters using multibeam acoustic data: A case study on the Carnarvon Shelf, Western Australian." International Journal of Geographical Information Science 26: 205-216.

Iampietro, P. J., Young, M.A., Kvitek, R.G. (2008). "Multivariate prediction of Rockfish habitat suitability in Cordell Bank National Marine Sancturary and Del Monte Shalebeds, California, USA." Marine Geodesy 31: 359-371.

Jenness, J. S. (2004). "Calculating landscape surface area from digital elevation models. ." Wildlife Society Bulletin, 32: 829-839.

Jordan, A. R., M. Lawler, V. Halley and N. Barrett (2005). "Seabed habitat mapping in the Kent Group of Islands and its role in marine protected area planning." Aquatic Conservation: Marine and Freshwater Ecosystems 15: 51-70.

Kostylev, V. E., R. C. Courtney, G. Robert and B. J. Todd (2003). "Stock evaluation of giant scallop (Placopecten magellanicus) using high-resolution acoustics for seabed mapping." Fisheries Research 60(2-3): 479-492.

Kostylev, V. E., Erlandsson, J., Ming, M.Y., & Williams, G.A. (2005). "The relative importance of habitat complexity and surface are in assessing biodiversity: fractal application on rocky shores." Ecological Complexity 2: 272-286.

Lindsay, J. B. (2006). "Sensitivity of channel mapping techniques to uncertainty in digital elevation data." International Journal of Geographical Information Science 20(6): 669-692.

Liu, X., P. Hu, H. Hu and J. Sherba (2012). "Approximation Theory Applied to DEM Vertical Accuracy Assessment." Transactions in GIS 16(3): 397-410.

Lundblad, E. R., D. J. Wright, J. Miller, E. M. Larkin, R. Rinehart, D. F. Naar, B. T. Donahue, S. M. Anderson and T. Battista (2006). "A Benthic Terrain Classification Scheme for American Samoa." Marine Geodesy 29: 98-111.

Lurton, X. (2003). "Theoretical Modelling of Acoustical Measurement Accuracy for Swath Bathymetric Sonars." International Hydrographic Review **4**: 17-30.

Lurton, X. and J. M. Augustin (2010). "A Measurement quality factor for swath bathymetry sounders." IEEE Journal of Oceanic Engineering **35**: 852-862.

Lurton, X., Y. Ladroit and J.-M. Augustin (2012). A Quality Estimator of Acoustic Sounding Detection. The International Hydrographic Review. Monaco, International Hydrographic Bureau.

Manly, B. F. J. (1997). Randomisation, Bootstrap, and Monte Carlo Methods in Biology, 2nd edn. London, Chapman & Hall.

Mateo Sánchez, M. C., S. A. Cushman and S. Saura (2013). "Scale dependence in habitat selection: the case of the endangered brown bear (Ursus arctos) in the Cantabrian Range (NW Spain)." International Journal of Geographical Information Science 28(8): 1531-1546.

McArthur, M. A., B. P. Brooke, R. Przeslawski, D. A. Ryan, V. L. Lucieer, S. Nichol, A. W. McCallum, C. Mellin, I. D. Cresswell and L. C. Radke (2010). "On the use of abiotic surrogates to describe marine benthic biodiversity." Estuarine, Coastal and Shelf Science 88(1): 21-32.

McBreen, F., Askew, N., Cameron, A., Connor, D., Ellwood, H., Carter, A., (2011). UKSeaMap 2010: Predictive Mapping of Seabed Habitats in UK Waters. J. N. C. Committee. Report, No. 446.

Mellin, C., S. Delean, J. Caley, G. Edgar, M. Meekan, R. Pitcher, R. Przeslawski, A. Williams and C. Bradshaw (2011). "Effectiveness of Biological Surrogates for Predicting Patterns of Marine Biodiversity: A Global Meta-Analysis." PLoS ONE 6(6): e20141.

Monk, J., D. Ierodiaconou, E. Harvey, A. Rattray and V. L. Versace (2012). "Are We Predicting the Actual or Apparent Distribution of Temperate Marine Fishes?" PLoS ONE 7(4): e34558.

Moore, I.D., Grayson, R.B. and Landson, A.R. (1991). “Digital Terrain Modelling: A review of hydrological, geomorphological, and biological application” Hydrological Processes 5: 3-30.

Mosher, D. C. (2011). "Cautionary considerations for geohazard mapping with multibeam sonar: resolution and the need for the third and fourth dimensions." Marine Geophysical Research 32: 25-35.

Nichol, S. L., Howard, F.J.F., Kool, J., Stowar, M., Bouchet, P., Radke, L., Siwabessy, J., Przeslawski, R., Pichard, K., Alvarez de Glasby, B., Colquhoun, J., Letessier, T., Heyward, A.,

(2013). Oceanic Shoals Commonwealth Marine Reserve (Timor Sea) Biodiversity Survey:. GA0339/SOL5650 – Post Survey Report. Record 2013/38. . Canberrra., Geoscience Australia.

Oksanen, J. and T. Sarjakoski (2005). "Error propagation of DEM-based surface derivatives." Computers & Geosciences(31): 1015-1027.

Oksanen, J. and T. Sarjakoski (2006). "Uncovering the statistical and spatial characteristics of fine toposcale DEM error." International Journal of Geographical Information Science 20(4): 345-369.

Openshaw, S., Charlton, M., & Carver, S. (1991). Error propagation: a Monte Carlo simulation. Handling Geographical Information. In I. Masser & M. Blakemore (Eds.). Harlow, Longman: 78-101.

Rengstorf, A. M., A. Grehan, C. Yesson and C. Brown (2012). "Towards High-Resolution Habitat Suitability Modeling of Vulnerable Marine Ecosystems in the Deep-Sea: Resolving Terrain Attribute Dependencies." Marine Geodesy 35(4): 343-361.

Shary, P. A., L. S. Sharaya, and A. Mitusov (2002). "Fundamental quantitative methods of land surface analysis." Geoderma **107**: 1-32.

Taylor, J. R. (1982). An introduction to error analysis: the study of uncertainties in physical measurements. . Mill Valley, California, University Science Books.

Vasquez, M. E. (1999). Tuning the CARIS implementation of CUBE for Patagonian Waters. Master of Science in Engineering, The University of New Brunswick.

Wilson, M., B. O'Connell, C. Brown, J. C. Guinan and A. J. Grehan (2007). "Multiscale terrain analysis of multibeam bathymetry data for habitat mapping on the continental slope." Marine Geodesy 30: 3-35.

Yesson, C., M. L. Taylor, D. P. Tittensor, A. J. Davies, J. Guinotte, A. Baco, J. Black, J. M. Hall-Spencer and A. D. Rogers (2012). "Global habitat suitability of cold-water octocorals." Journal of Biogeography 39(7): 1278-1292.

Table 1: The 28 levels of depth uncertainty and their values; increased from nadir (U_1) to outer beam (U_{28}).

Uncertainty Level	Uncertainty Value[1]	Highest Possible Uncertainty[2]	Frequency	Uncertainty Level	Uncertainty Value	Highest Possible Uncertainty	Frequency
U_1	0.31	0.80	17.79	U_2	0.32	0.83	8.26
U_3	0.33	0.85	5.98	U_4	0.34	0.88	6.48
U_5	0.35	0.90	5.46	U_6	0.36	0.93	4.66
U_7	0.37	0.95	4.96	U_8	0.38	0.98	5.17
U_9	0.39	1.01	4.01	U_{10}	0.40	1.03	4.19
U_{11}	0.41	1.06	4.30	U_{12}	0.42	1.08	3.30
U_{13}	0.43	1.11	3.44	U_{14}	0.44	1.14	3.43
U_{15}	0.45	1.16	2.47	U_{16}	0.46	1.19	2.40
U_{17}	0.47	1.21	2.45	U_{18}	0.48	1.24	2.21
U_{19}	0.49	1.26	3.03	U_{20}	0.50	1.29	3.23
U_{21}	0.51	1.32	1.75	U_{22}	0.52	1.34	0.82
U_{23}	0.54	1.39	0.10	U_{24}	0.55	1.42	0.07
U_{25}	0.56	1.44	0.04	U_{26}	0.57	1.47	0.004
U_{27}	0.58	1.50	0.0008	U_{28}	0.60	1.55	0.00002

Note:

[1] represented as 1 standard deviation of the uncertainty distribution;

[2]Calculated at 99% confidence interval

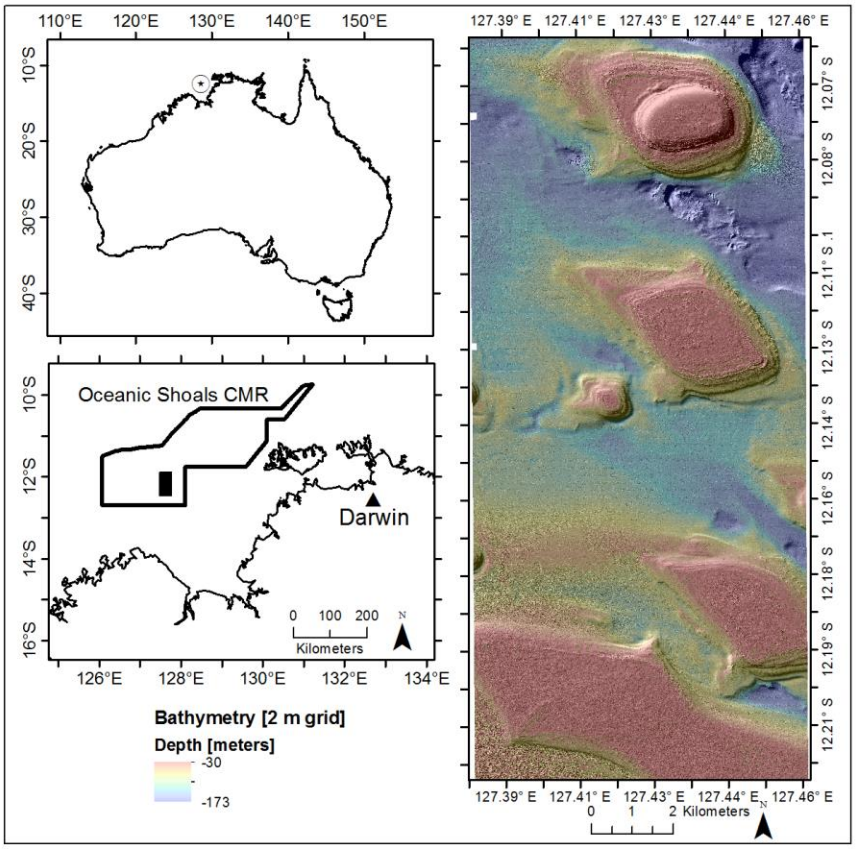

Figure 1. Location of the study area to the North West of Australia and the bathymetry grid obtained from the CUBE algorithm.

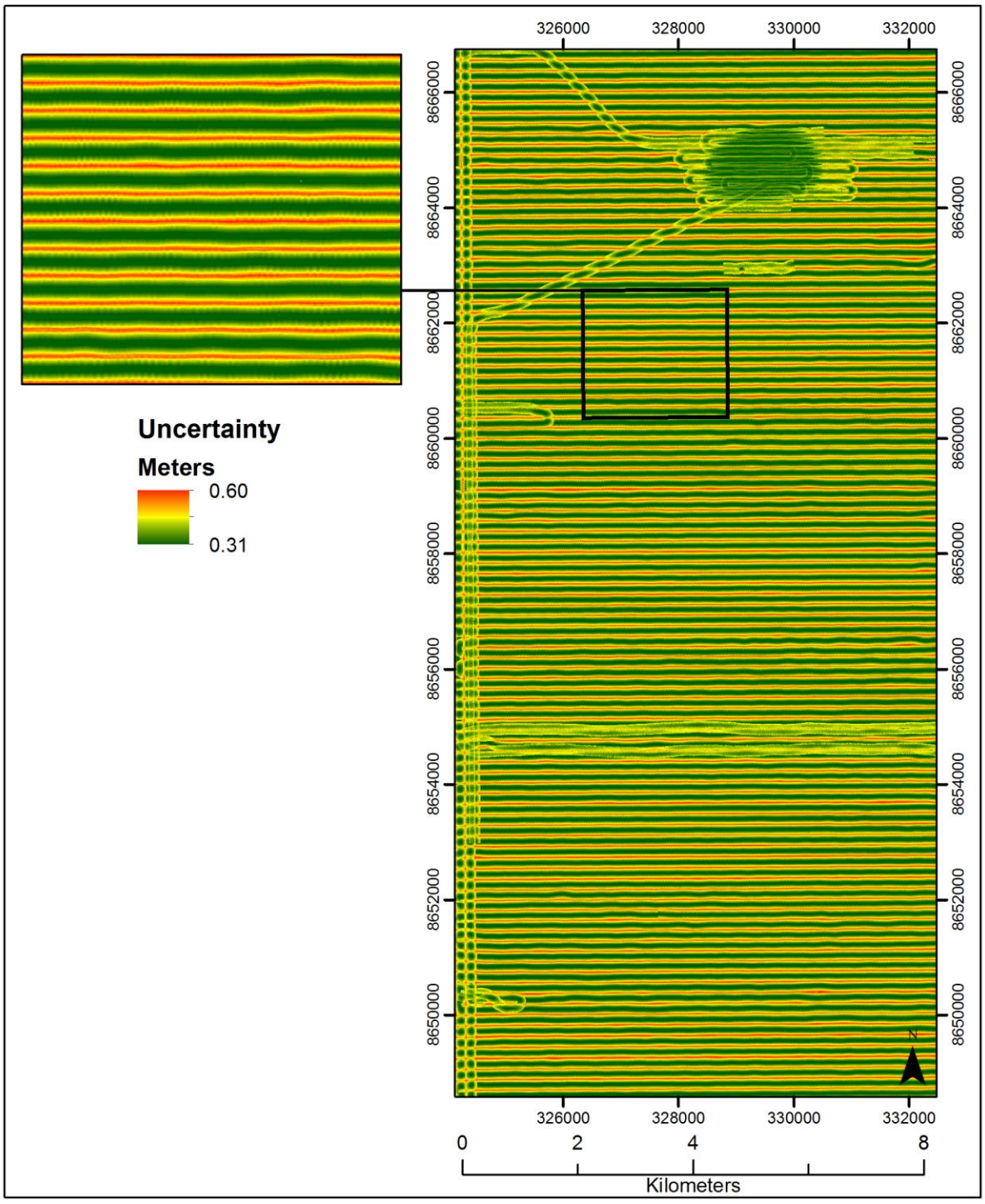

Figure 2. The original uncertainty layer obtained from the CUBE algorithm. Highest uncertainty (red) is located in the outer beams and lowest uncertainty (green) is located closer to nadir. The value indicates one standard deviation of the Gaussian uncertainty distribution (mean=0).

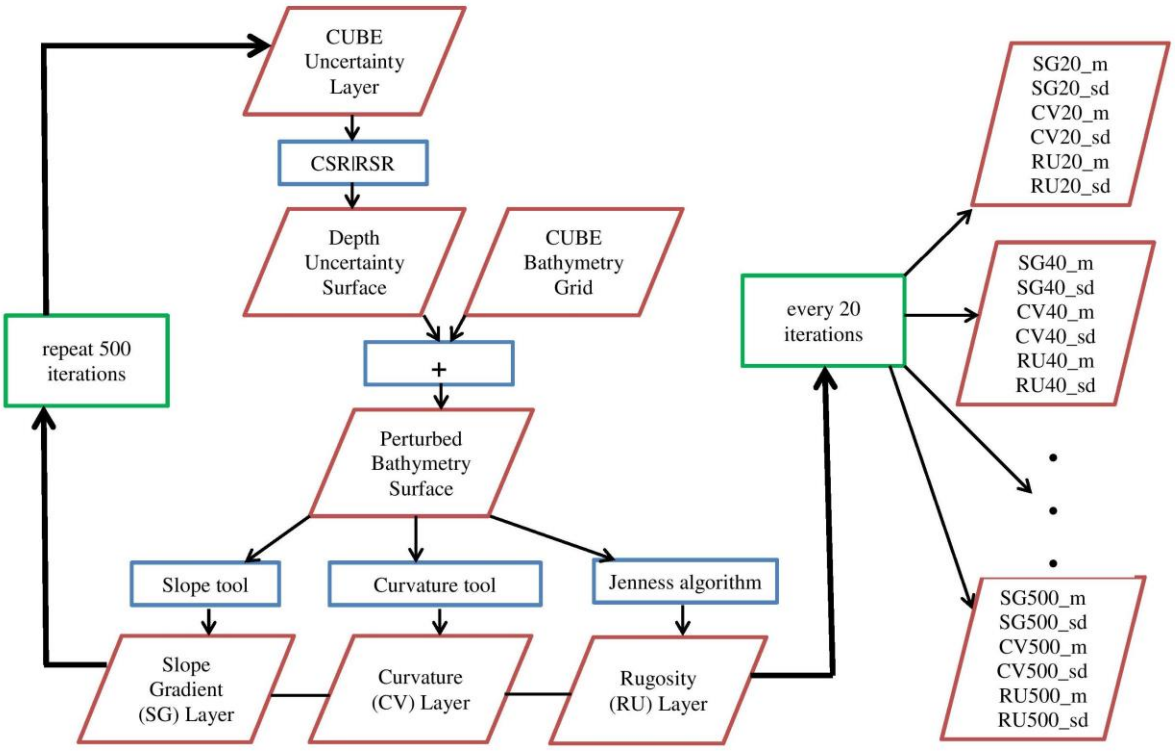

Figure 3. The diagram explains how the Monte Carlo simulation procedure is used in this study.

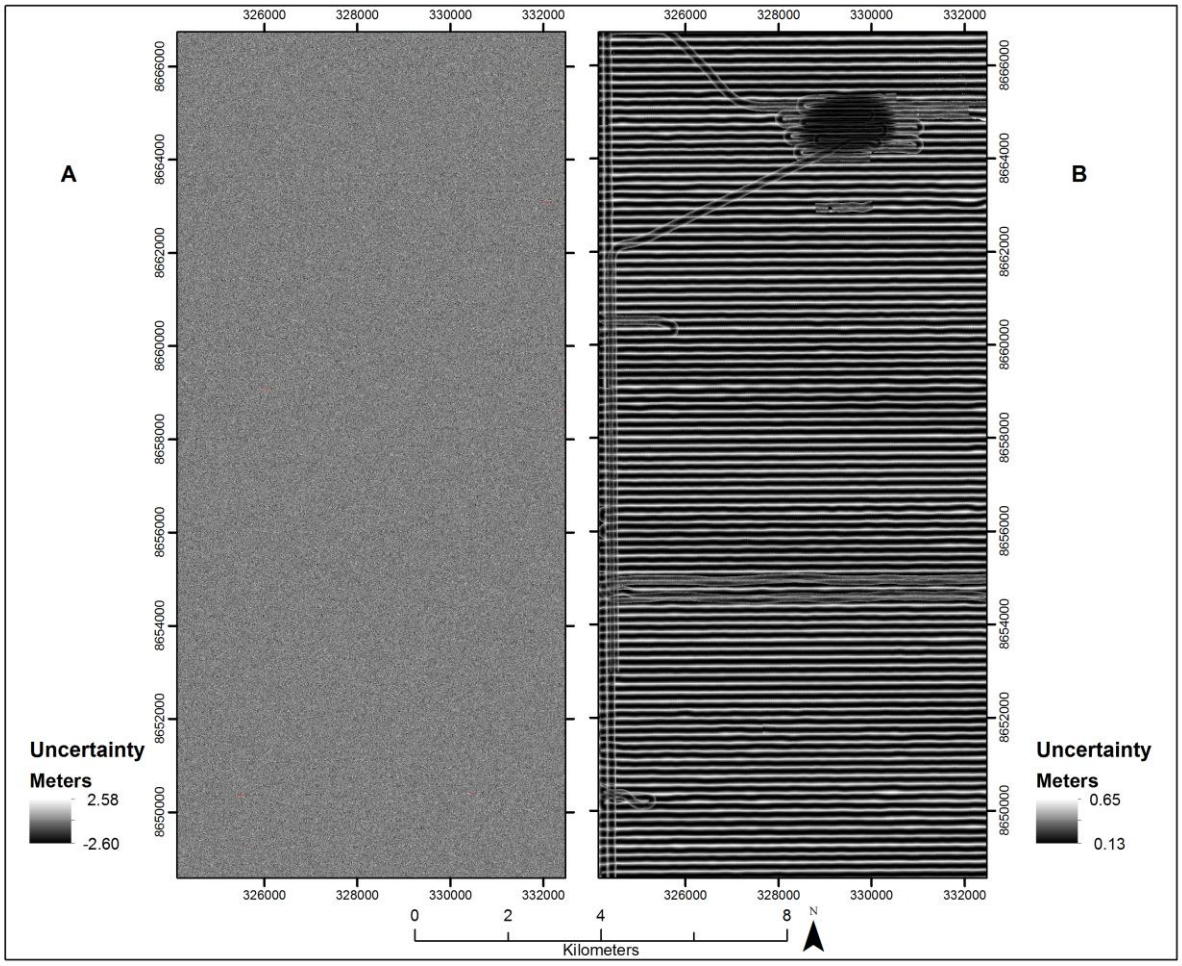

Figure 4. The constructed depth uncertainty surfaces at the 100th iteration; (A) the CSR method; (B) the RSR method. The value indicates simulated offset (error) from the true depth.

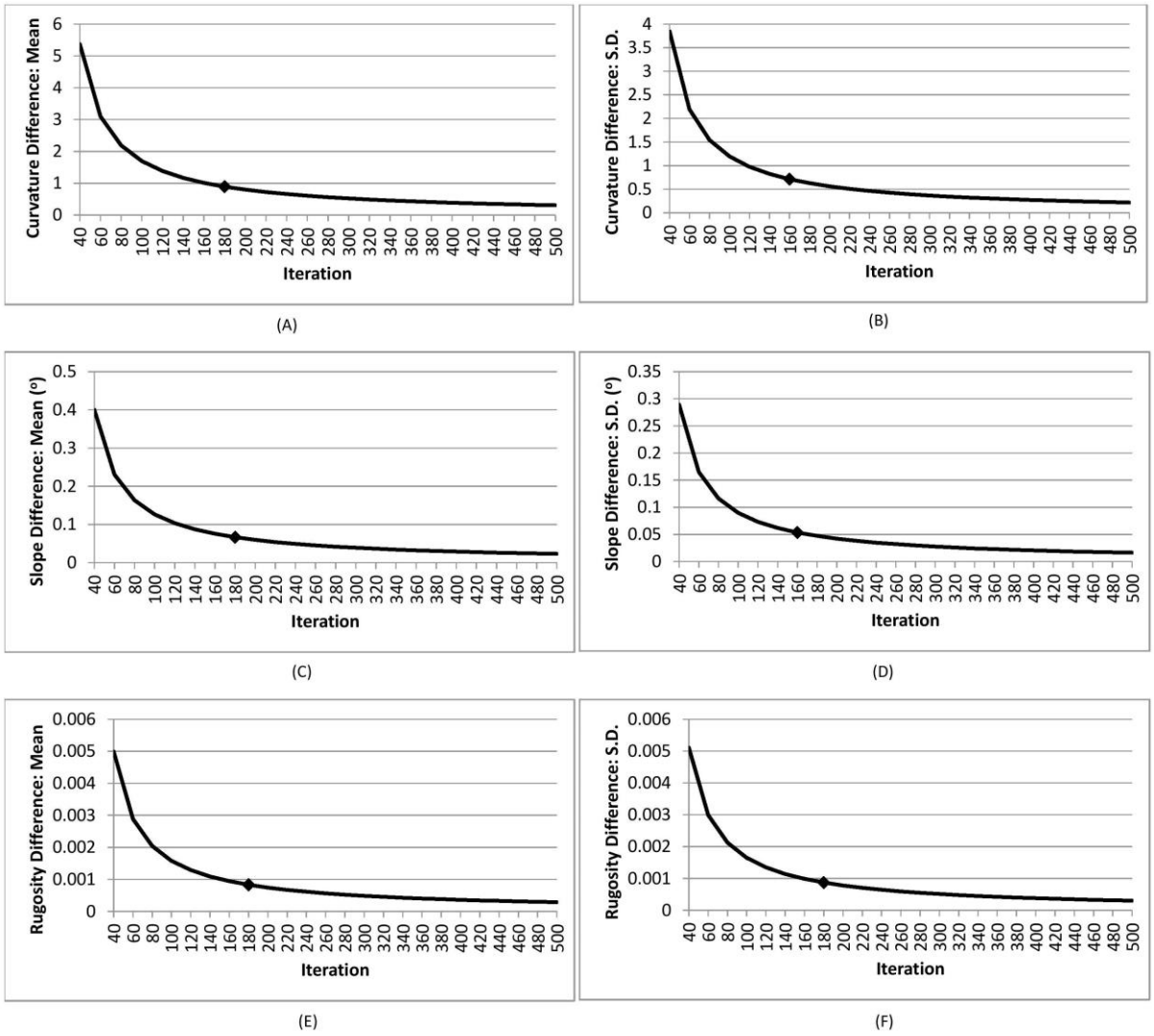

Figure 5. The Monte Carlo convergence lines for the CSR method; (A) the mean statistic for the curvature variable; (B) the standard deviation statistic for the curvature variable; (C) the mean statistic for the slope gradient variable; (D) the standard deviation statistic for the slope gradient variable; (E) the mean statistic for the rugosity variable; (F) the standard deviation statistic for the rugosity variable. The black dots indicate the convergence points.

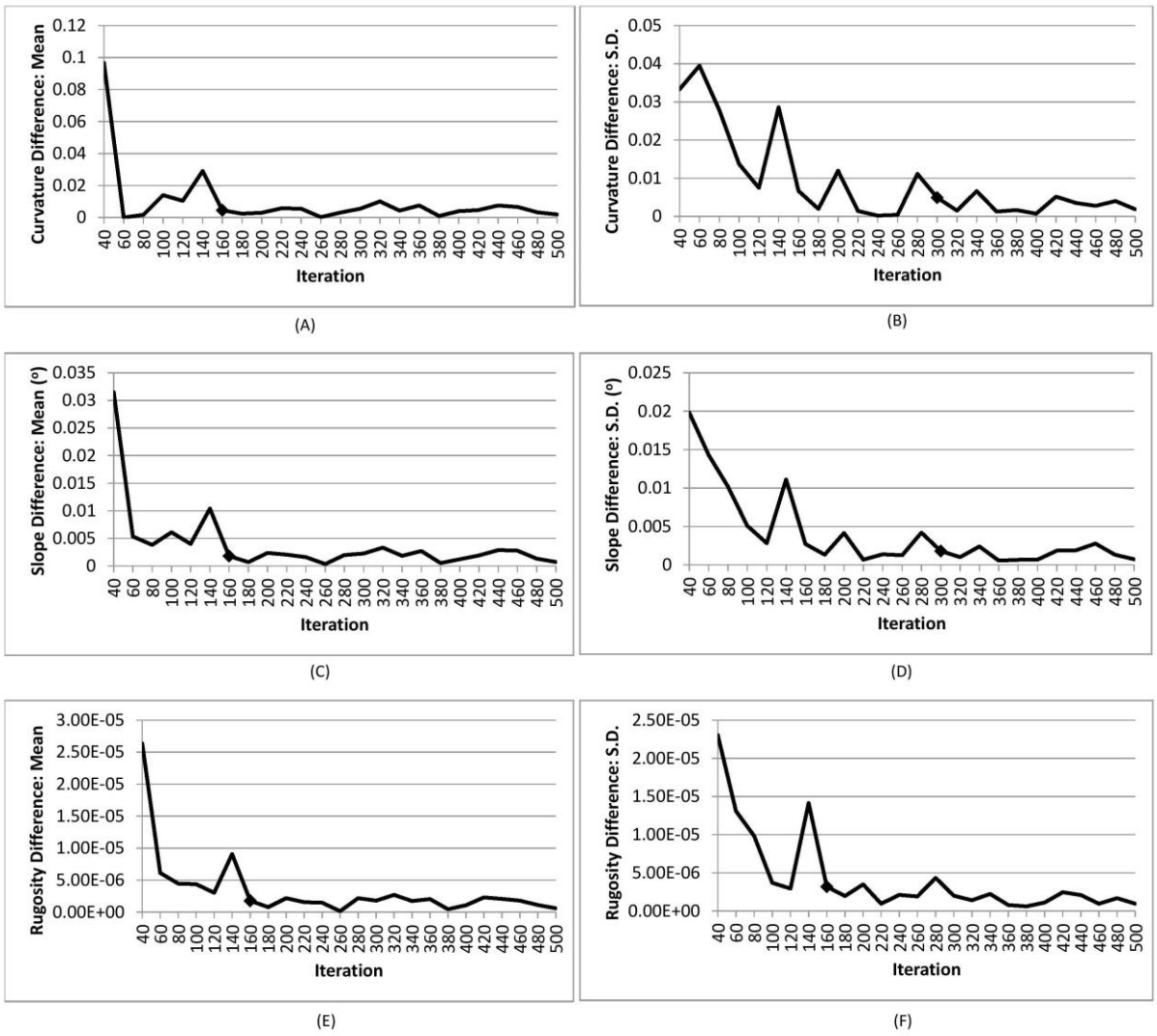

Figure 6. The Monte Carlo convergence lines for the RSR method; (A) the mean statistic for the curvature variable; (B) the standard deviation statistic for the curvature variable; (C) the mean statistic for the slope gradient variable; (D) the standard deviation statistic for the slope gradient variable; (E) the mean statistic for the rugosity variable; (F) the standard deviation statistic for the rugosity variable. The black dots indicate the convergence points.

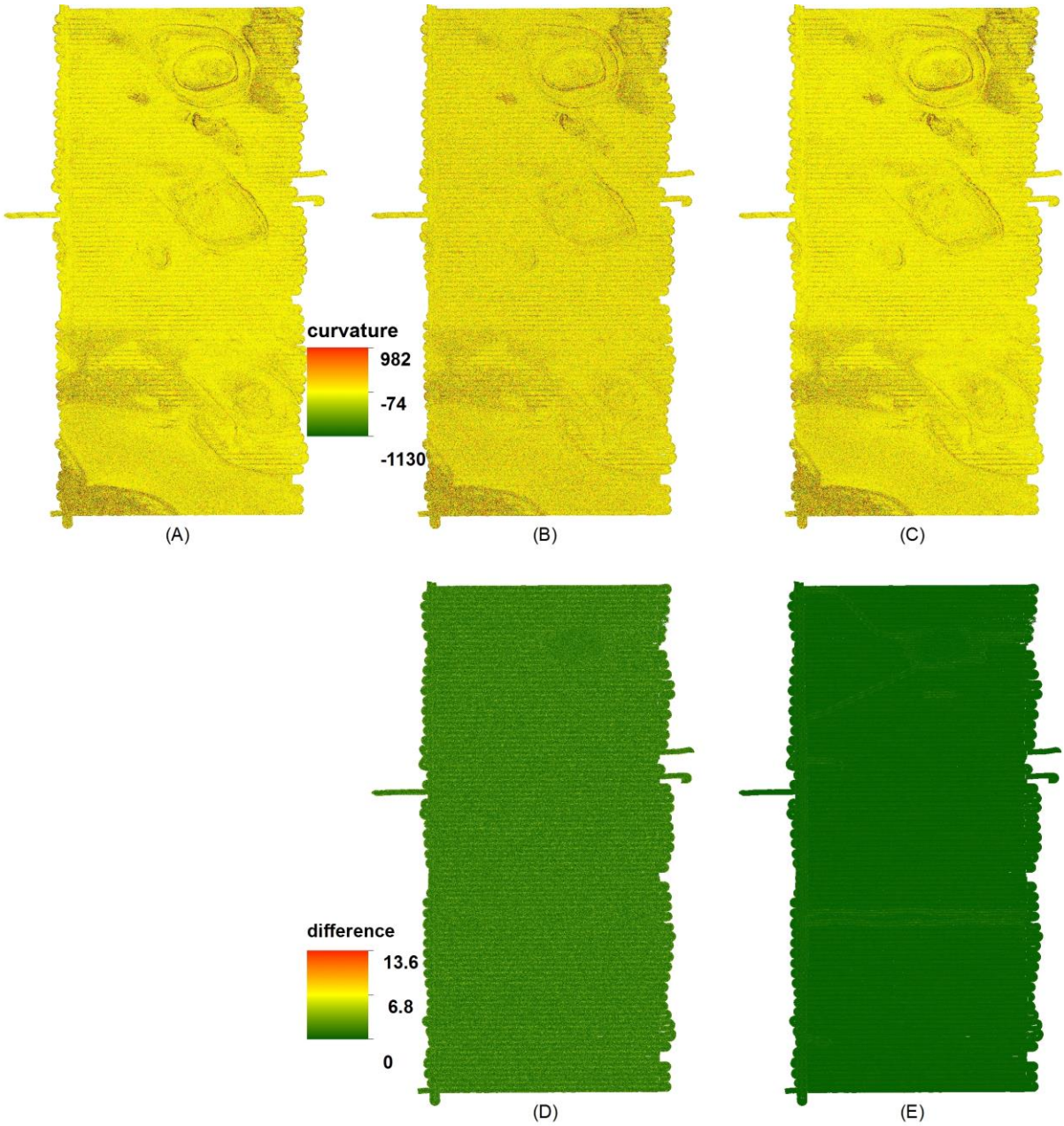

Figure 7. The Monte Carlo simulation results for the curvature variable; (A) derived from the unperturbed bathymetry grid (RU); (B) the mean layer after 500 iterations of the CSR method; (C)) the mean layer after 500 iterations of the RSR method; (D) the absolute difference between B and A; (E) the absolute difference between C and A.

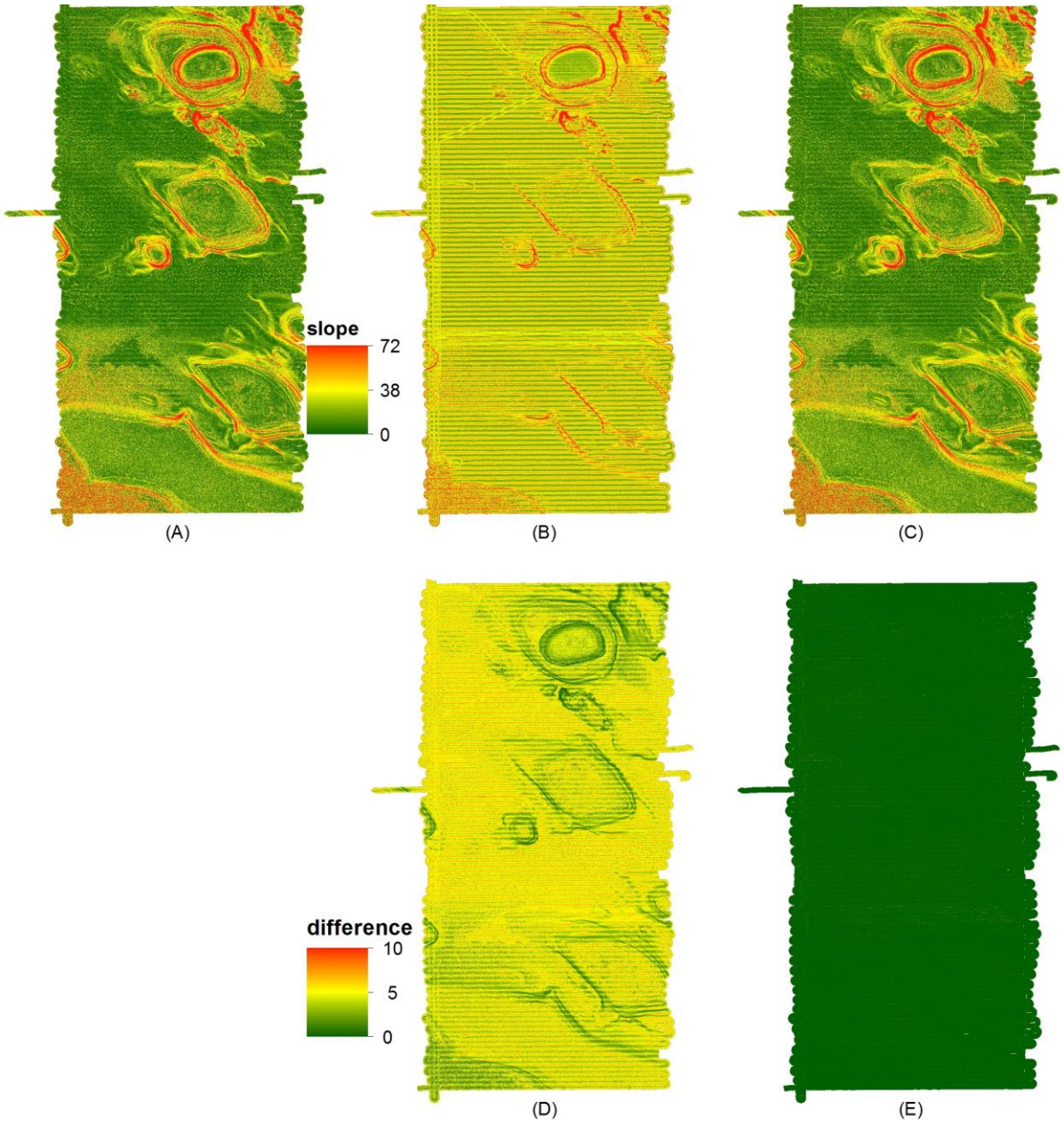

Figure 8. The Monte Carlo simulation results for the slope gradient variable; (A) derived from the unperturbed bathymetry grid (RU); (B) the mean layer after 500 iterations of the CSR method; (C)) the mean layer after 500 iterations of the RSR method; (D) the absolute difference between B and A; (E) the absolute difference between C and A.

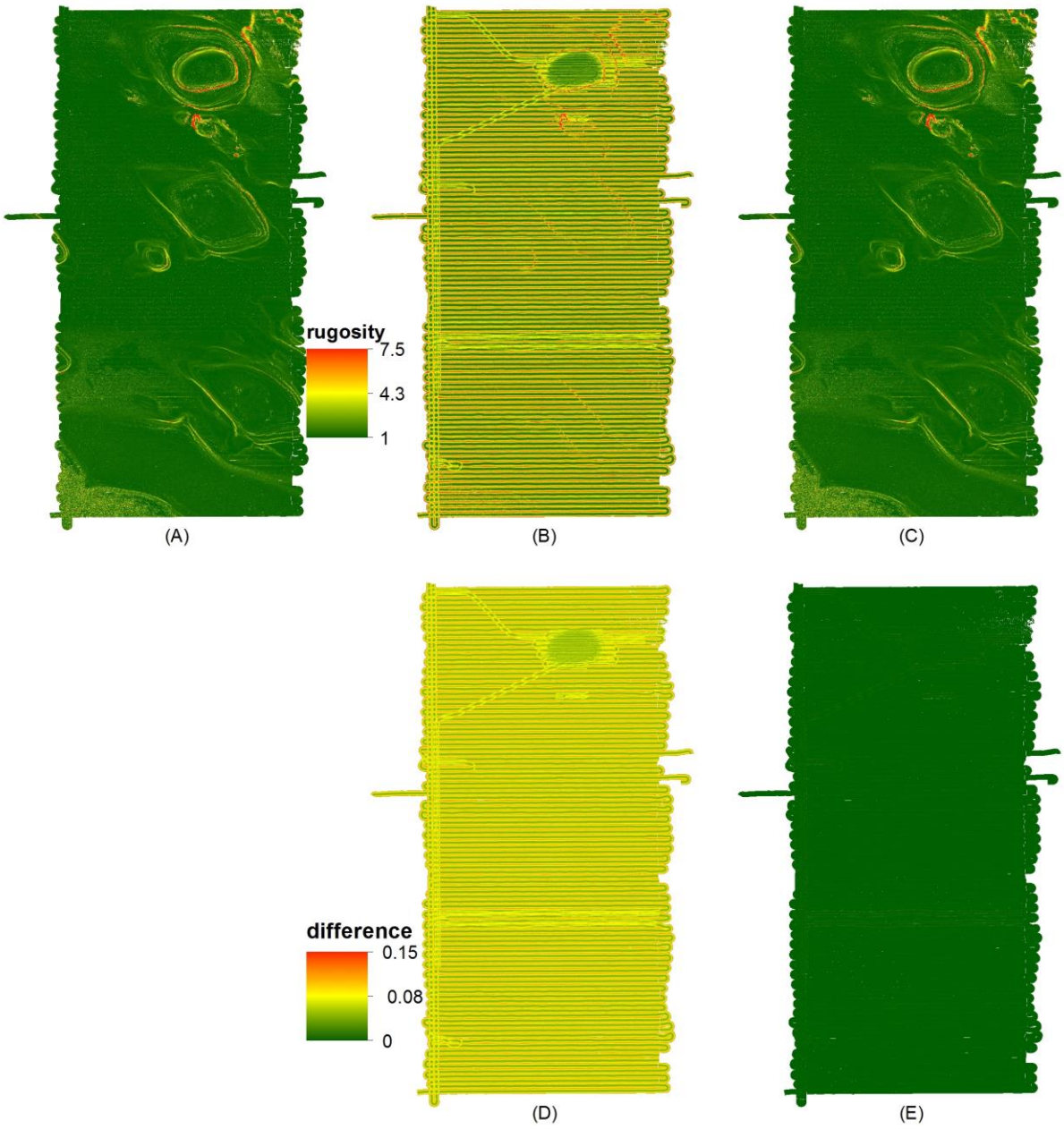

Figure 9. The Monte Carlo simulation results for the rugosity variable; (A) derived from the unperturbed bathymetry grid (RU); (B) the mean layer after 500 iterations of the CSR method; (C)) the mean layer after 500 iterations of the RSR method; (D) the absolute difference between B and A; (E) the absolute difference between C and A.